Two-Color Ultrafast Photoexcited Scanning Tunneling Microscopy

ARTICLE *in* THE JOURNAL OF PHYSICAL CHEMISTRY C · APRIL 2011

Impact Factor: 4.77 · DOI: 10.1021/jp111875f

THE JOURNAL OF PHYSICAL CHEMISTRY C

ARTICLE

pubs.acs.org/JPCC

Two-Color Ultrafast Photoexcited Scanning Tunneling Microscopy

A. Dolocan,[†,§] D. P. Acharya,[‡,∥] P. Zahl,[‡] P. Sutter,[‡] and N. Camillone, III[*,†]

[†]Chemistry Department and [‡]Center for Functional Nanomaterials, Brookhaven National Laboratory, Upton, New York 11973, United States

ABSTRACT: We report on two-color two-photon photoexcitation of a metal surface driven by ultrafast laser pulses and detected with a scanning tunneling microscope (STM) tip as a proximate anode. Results are presented for two cases: (i) where the tip is retracted from the surface far enough to prohibit tunneling, and (ii) where the tip is within tunneling range of the surface. A delay-modulation technique is implemented to isolate the two-color photoemission from concurrent one-color two-photon photoemission and provide subpicosecond time-resolved detection. When applied with the tip in tunneling range, this approach effectively isolates the two-photon photoexcited current signal from the conventional tunneling current and enables subpicosecond time-resolved detection of the photoexcited surface electrons. The advantage of the two-color approach is highlighted by comparison with the one-color case where optical interference causes thermal modulation of the STM tip length, resulting in tunneling current modulations that are orders of magnitude larger than the current due to photoexcitation of surface electrons. By completely eliminating this interference, and thereby avoiding thermal modulation of the STM tip length, the two-color approach represents an important step toward the ultimate goal of simultaneous subnanometer and subpicosecond measurements of surface electron dynamics by ultrafast-laser-excited STM.

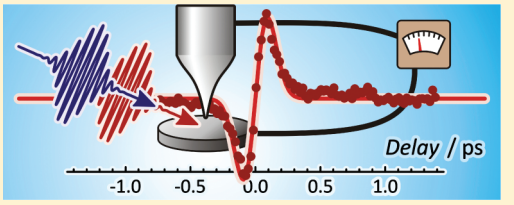

1. INTRODUCTION

Surface chemistry, by definition, is a local ultrafast phenomenon: surface chemical transformations involve subnanometer-scale electronic and nuclear motions at femtosecond to picosecond time scales. Substrate−adsorbate energy transfer mediated by surface electronic excitations is central to photoinduced surface chemistry,[1] and its significance in thermal chemistry at metal surfaces is becoming increasingly appreciated.[2−4] However, direct observation of the effects of surface inhomogeneity (e.g., surface defects, nanostructures) on charge carrier dynamics, and their correlation to (photo)reactivity, remains a challenge. To enable investigation of the role of local electronic excitations in surface chemical and photochemical processes at the atomic level, we are developing a laser-excited scanning tunneling microscopy approach to probing subpicosecond hot-carrier dynamics with near-atomic resolution.

Almost since the invention of the scanning tunneling microscope (STM),[5] the idea of observing laser-stimulated phenomena with atomic resolution has been pursued.[6] Because the STM is sensitive to local surface electron densities, it is logical to consider using the STM to spatially resolve electronic excitations driven by ultrafast laser pulses. Photoexcitation generates a distribution of excited electrons (holes) in states above (below) the Fermi level, and should result in time-dependent changes in the tunneling probability that reflect the local electronic excitation and relaxation dynamics at the surface. However, the shortest response time of an STM—limited by the ∼100-kHz bandwidth of the current-to-voltage converter—is ∼8 orders of magnitude too slow to directly detect subpicosecond transients associated with hot-carrier relaxation in metals. Thus, to time resolve local electron dynamics, various ultrafast-laser pump−probe schemes have been proposed and attempted.[7−11] Recent work has suggested that subpicosecond laser excitation of the tip−surface junction may enable ultrafast probing of surface electron dynamics with subnanometer spatial resolution.[11−17] However, to date, conclusive evidence of simultaneous subpicosecond- and subnanometer-resolved measurements of surface electron dynamics has not been shown.

Direct pulsed-laser excitation of the tunneling junction is attractive because it offers a general approach applicable to a broad range of surfaces and avoids complications such as the capacitive coupling that limits the spatial resolution in photoconductively gated STM to the micrometer scale.[18] However, as shown by Grafström and co-workers,[19,20] Pfeiffer and co-workers,[21] Yates and co-workers,[22,23] and others,[24] pulsed-laser excitation of the STM tip is accompanied by thermal expansion which results in a strong modulation of the tunneling current due to the exponential dependence of the current on the tip−surface separation. Such thermal expansion effects are expected to predominate over effects due to hot-carrier dynamics and conceal the signals of interest.[25] The magnitude of the thermal expansion can be mitigated by using a high-repetition-rate laser.[11,20] However, calculations predict that a tungsten tip responds to picosecond pulsed laser excitation on a ∼1-ns time scale,[21] and therefore, even excitation at ∼100-MHz repetition rates is not reliably approximated by continuous-wave heating. Consequently, a means for extracting the desired signal (due to the electronic response) from the undesired signal (due to thermal effects) is required.

In principle, ultrafast-laser-based two-pulse correlation (2PC) methods address both the slow detection response of the STM

Received: December 14, 2010
Revised: March 18, 2011
Published: April 27, 2011

and the thermal response of the tip. In a one-color 2PC experiment, the excitation pulse is split into two pulses separated in time by a variable delay; the delay is varied by controlling the difference in path lengths that the two pulses traverse, and a slow detector is used to measure the response of the target system as a function of the delay between the pulses. This approach is motivated by the fact that the degree of electronic excitation depends on the delay between the two pulses:[12,26] two subpicosecond pulses arriving at the same time (or with a delay of the order of the electron−phonon coupling time[27]) excite the system more strongly than two pulses separated by a large (generally >1 ps) delay. Thus, by measuring a time-averaged observable (i.e., the tunneling current) as a function of the delay, in principle, the overall relaxation of the electron distribution can be determined. In the application of such an approach to ultrafast photoexcited STM, the time resolution would be limited by the temporal width of the laser pulses, not by the bandwidth of the STM electronics, and furthermore, subpicosecond transients would be easily distinguished from the ∼1-ns thermal response. Two groups have explored the application of ultrafast laser one-color 2PC approaches to time resolving surface electron dynamics in the STM by direct laser excitation of the tunneling gap: Pfeiffer and co-workers[25] and Shigekawa and co-workers.[12,16,17] Very recently Wu and Ho have explored the application of a 2PC approach to time resolving electron transfer from the tip to an adsorbate.[28] The relationship of this work to our present effort is considered in more detail below (see Results and Discussion). Here we restrict our introductory remarks to experiments aimed at simultaneous subnanometer and subpicosecond investigations of electron dynamics at the substrate surface.

Pfeiffer and co-workers found that the intensity modulation that occurs due to the optical interference between two ultrafast pulses of identical wavelength overlapped in time at the tip−surface junction results in a strong variation of the width of the tunneling gap.[25] With 12 mW of the output of an 800-nm, 80-MHz, 40-fs Ti:sapphire oscillator focused to a 50-μm spot, they observed a peak-to-peak tunneling-gap modulation greater than 1 nm. Given (i) the ∼10-fold increase in tunneling current for every angstrom decrease in the tunnel-gap width, and (ii) the low levels expected for the photoinduced tunneling currents, where only a very small minority of the tunneling electrons are due to photoexcitation (a current estimated to be ∼5 orders of magnitude smaller than the normal tunneling current, given the brevity of the ∼1-ps excitation compared to the ∼10-ns period between the pulses), such a tunneling-gap modulation would introduce currents so large that extraction of the desired signal at time delays of the order of the laser pulse temporal width would be impossible.

To eliminate the current modulation resulting from thermal expansion and contraction of the STM tip, Shigekawa and co-workers proposed a modified technique, which they called "shaken-pulse-pair-excited" (SPPX) STM.[11,12] In SPPX-STM, the delay between the pulses is dithered sinusoidally at a frequency in the 10−100 Hz range, and phase-sensitive lock-in amplification is employed to detect the signal at the modulation frequency. The approach is well-suited to detecting small signal differences in the presence of a large background, such as those expected in an ultrafast-pulse-excited STM. Shigekawa and co-workers proposed that SPPX-STM with a high (megahertz) repetition rate laser should eliminate the thermal-expansion-driven modulation of the STM tunneling gap width that has historically hindered laser-excited STM.[11,12,14,29] Indeed, their method shows promise for time resolving phenomena in the 10−1000 ps range[16] and has recently been modified (see Results and Discussion) to reach the microsecond regime.[30] However, the results of our one-color 2PC measurements reported here, in accord with those of Pfeiffer and co-workers,[25] indicate that, as implemented, the one-color SPPX approach does not provide a measure of the subpicosecond dynamics. To be more specific, one-color results show that optical interference (at delay times of the order of the sum of the temporal widths of the laser pulses and the dither amplitude) drives strong thermal expansion and contraction of the STM tunneling gap width and creates a "blind spot" of ∼1 ps in previously reported experiments.[14]

In this paper we present results that illustrate the magnitude of the problem inherent in making one-color 2PC measurements in the STM, showing that optical interference results in thermal fluctuations that are too large to ignore when attempting to resolve surface dynamics on the time scale of the laser pulse. We then detail our approach to eliminating the thermal modulation of the STM tip length caused by optical interference. Specifically, we describe our two-color pump−probe approach. As an initial step, we employ the near infrared (NIR) fundamental (photon energy ∼1.6 eV) and ultraviolet A (UVA) second harmonic (∼3.2 eV) of a Ti:sapphire oscillator to excite electrons at a Ag(111) surface (work function = 4.5 eV[31,32]). Thus a minimum of two photons—either one each of the two colors (NIR + UVA) or two of a single color (2 × UVA)—are required for photoemission. We detect the photoemission with the STM tip under two conditions: (i) where the tip is retracted from the surface far enough to prohibit tunneling (and minimize tip-induced optical field enhancement at the surface), and (ii) where the tip is within tunneling range of the surface (opening up the possibility for photoassisted tunneling of subvacuum hot electrons to contribute to the current). We show that the two-color pump−probe approach eliminates optical interference both when the tip is retracted (as expected) and when the tip is in tunneling range. We demonstrate time-resolved measurements achieved through implementation of the delay-dithering technique that isolates the two-color photoemission from concurrent one-color two-photon photoemission. These results represent an important step toward the ultimate goal of simultaneous subnanometer and subpicosecond measurements of surface electron dynamics.

2. EXPERIMENTAL METHODS

The design of our laser-assisted STM setup addresses the key issues that have historically hampered progress: vibration, thermal drift, photoinduced thermal expansion, and optical interference. To hold the laser alignment and thermal load on the STM tunneling gap fixed, our setup incorporates active vibration cancellation and a closed-loop electro-optic-modulator laser-power stabilizer. To minimize thermal drift and provide for stringent control over the conditions at the surface, we employ a cryogenic ultrahigh vacuum (UHV) STM (Createc LT-STM, base pressure $<1 \times 10^{-10}$ Torr, base temperature ∼5 K). We use electrochemically etched tungsten STM tips for both topographic imaging and the ultrafast-laser-driven photoexcitation measurements.

The laser source is a high repetition rate (∼80 MHz), ∼80-fs pulse, high-power (∼2.7 W at 800 nm) Ti:sapphire oscillator tunable in the 730−850 nm range (Spectra-Physics Tsunami). The temporal width of the NIR pulses at the sample surface is

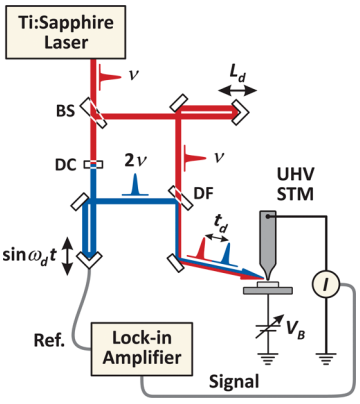

Figure 1. Simplified schematic of the two-color cross-correlation laser-excited STM setup. The femtosecond mode-locked Ti:sapphire oscillator output is split by a beam sampler (BS): ∼90% of the NIR (ν) fundamental is frequency doubled in an LBO crystal (DC) in one arm of the modified Mach−Zehnder interferometer; the ∼5% reflected from one face of the sampler traverses the other arm of the interferometer; the remaining ∼5% reflected from the other face of the sampler can be used for diagnostics (not shown). The UVA (2ν) generated in the doubling crystal traverses an optical delay line whose length is modulated by applying a sinusoidal dither ($\sin \omega_d t$) to a piezoelectric-driven translation stage (300-μm maximum travel) on which a retroreflector is mounted. The NIR beam traverses a second variable optical delay line comprised of a retroreflector mounted on a linear translation stage (16-cm maximum travel). The two colors are recombined on a dichroic filter (DF) and focused onto the tip−surface junction. The current (I) across the junction is monitored (after amplification in a current-to-voltage converter) simultaneously (i) by lock-in amplification at the frequency of the sinusoidal dither and (ii) without further modification by the STM control electronics.

estimated to be ∼100 fs (full width at half-maximum, fwhm) based on autocorrelation measurements performed external to the UHV chamber on an optical path similar to that traversed by the beams incident on the sample. The UVA light is produced by type I critically phase matched second-harmonic generation in a lithium triborate (LBO, 1 mm thick) crystal. The temporal width of the UVA pulses at the sample is estimated to be ∼190 fs (fwhm) based on the ∼215-fs fwhm temporal width of the two-color two-photon photoemission (discussed below) and the ∼100-fs fwhm of the NIR pulses.

Our time-resolved measurements employ a modified Mach−Zehnder optical interferometer based on the SPPX concept.[11,12] The two-color setup is illustrated schematically in Figure 1. After the oscillator output passes through (i) sampling for temporal-width and spectrum analysis measurements, (ii) a zero-order half-wave plate and polarizer for power adjustment, and (iii) the electrooptic power stabilizer (not shown in Figure 1), it is split into three beams by a wedged beam sampler. The ∼90% of the full beam transmitted by the sampler is sent to the doubling crystal to generate the UVA light. Approximately 5% of the beam is reflected into a two-prism group-velocity dispersion (GVD) compensation setup (not shown in Figure 1); after compensation this beam is directed into the NIR leg of the interferometer. A second reflected ∼5% (not shown in Figure 1) can be used for diagnostic purposes. The polarization of the NIR beam is rotated 90° so that it enters the GVD compensator with its electric field vector horizontal (such that it is incident on the prism faces with p-polarization). The second harmonic generated by vertically polarized NIR in the LBO emerges naturally with a horizontal polarization. Thus both colors traverse the remainder of the interferometer with their polarizations horizontal. The optical path lengths of the SPPX interferometer arms are defined by the positions of two hollow first-surface-mirror retroreflectors, and are varied independently. The NIR-arm retroreflector is translated in discrete steps and held stationary for a specified "dwell time" at each step while the signal is recorded. The path length traversed by the UVA light is modulated sinusoidally with dither frequency, ω_d, and peak-to-peak amplitude, Δt_d, by modulating the position of the UVA-arm retroreflector with a piezoelectric-driven translation stage. Thus, the time-dependent optical delay is

$$t_d(t) = t_{dc}(t) + \Delta t_d \sin(\omega_d t) \quad (1)$$

where t is the laboratory-frame time and t_{dc} is the center value of the delay determined by the position of the NIR retroreflector. In the measurements reported here the NIR-retroreflector step size is 3 μm (corresponding to 20 fs optical delay), the dwell time is ∼1 s, $\omega_d/2\pi$ is 187 Hz, and Δt_d is ∼18.7 fs.

The parallel-polarized beams are recombined at the dichroic filter, and the two-color output of the interferometer is then focused to a spot size of approximately 20 μm × 100 μm with p-polarization on the sample surface under the STM tip. The length of the long axis of the elliptical spot is due to the shallow angle of incidence (∼78° with respect to the surface normal). The alignment of the laser focus to the tip apex is determined by visualization of the diffraction pattern collected after reflection from the sample, and confirmed by optimization of the photoemission current collected by the STM tip. Phase-sensitive detection of the tunneling current is achieved by driving the sinusoidal dither of the UVA-arm retroreflector with the amplified output of the internal oscillator of a digital lock-in amplifier; the internal oscillator also serves as the reference for the phase-sensitive detection. The output of the STM current-to-voltage converter (or "preamplifier") is fed into the lock-in amplifier, and the output of the lock-in amplifier is recorded on a personal computer.

3. RESULTS AND DISCUSSION

A. One-Color Two-Pulse Correlation. We begin by presenting data that illustrate the difficulty inherent in making STM-detected time-resolved measurements on time scales of the order of the temporal width of the laser pulse. Figure 2a shows an example of the strong modulation of the tunneling current that we observe in one-color 2PC experiments. In these experiments, the STM tunneling current is measured as a function of the delay between two essentially identical pulses (733-nm center wavelength), with the STM operated in constant-current mode (set point = 0.5 nA) and the response time of the height (z) servo loop set to 10 s. The tunneling current is averaged for ∼800 ms at each point; the points are separated by a change in the optical delay of 2 fs, and the delay is swept from point to point in fast jumps of the optical delay stage such that the current at each new delay position is measured after a very short time (∼10 ms) following the delay jump. Thus, though the feedback loop is set to maintain a constant tunneling current, changes in the tunneling current are readily detected during the time-delay sweep because they are fast compared to the slow response of the z servo loop. The incident fluence is ≅7 μJ cm^{-2} (per pulse), and the target surface is a clean, well-characterized rutile TiO_2(110)-(1 × 1) surface, chosen specifically to minimize optical absorption by the sample. The experimental laser setup

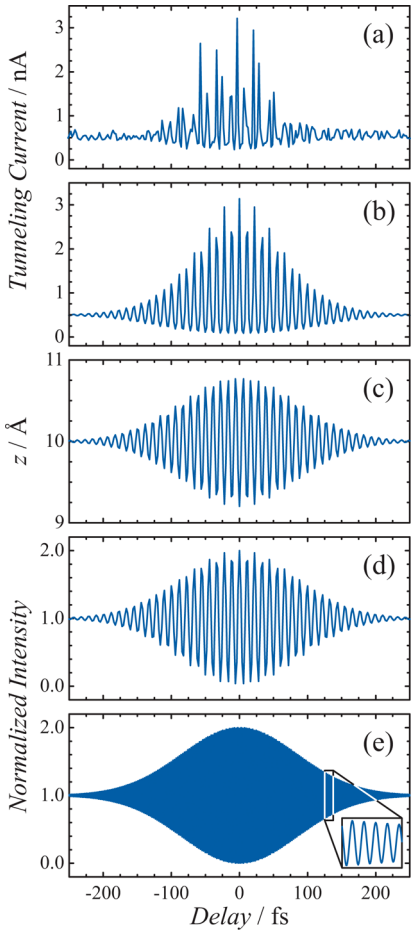

Figure 2. Measured (a) and simulated (b) effects of temporal interference on the current in a one-color two-pulse correlation experiment. The photoinduced thermal modulation of the apex height above the surface (c) and the corresponding linear interferogram for 100-fs fwhm NIR pulses [undersampled at 2.5-fs intervals (d) and with fully resolved fringes (e)] are also shown. The measurements were made on a TiO_2(110)-(1 × 1) surface with a tungsten tip and 733-nm pulses with an approximate per-pulse fluence of 7 μJ cm^{-2}. The pulses were perpendicularly polarized and fixed at ±45° relative to the surface normal. The STM was in constant-current mode (set point = 0.5 nA, sample bias = +1.3 V, feedback bandwidth setting = 0.1 Hz) and the temperature was ~80 K.

is the one-color equivalent of that depicted in Figure 1 with the following modifications: (i) a 50/50 beam splitter replaces the beam sampler, (ii) the laser pulses are cross polarized at ±45° relative to the STM tip axis in an attempt to minimize the interference effect described below, and (iii) because the observed effect near zero delay is large, there is no need to dither the delay or employ the lock-in amplifier; instead, we directly monitor the tunneling current.

We attribute the strong modulation of the tunneling current in Figure 2a to a corresponding thermal modulation of the STM tip length caused, in turn, by modulation of the optical power at the tunneling junction.[20,25] Figure 2e shows the delay-dependent interference calculated for two equal and parallel-polarized beams of 100-fs, 733-nm pulses. Near zero delay the light intensity is modulated from a minimum of zero (destructive interference) to a maximum equal to 4 times the intensity of one of the beams (constructive interference); far from zero delay, where there is negligible temporal overlap of the pulses and, therefore, negligible interference effects, the intensity is constant at a value equal to twice the intensity of a single beam. The fringes, shown in the inset of Figure 2e, occur with a period of 2.445 fs (i.e., λc^{-1}, where λ is the center wavelength of the subpicosecond pulse and c is the speed of light). In the experiment, the measurement is made at 2-fs intervals; Figure 2d is the same interference pattern shown in Figure 2e but sampled at 2-fs intervals. A simple but reasonable model of the response of the tip to this modulation of the laser intensity can be constructed from the well-known exponential dependence of the tunneling current on the tip−surface gap:

$$I = I_0 \exp(-z/z_0) \quad (2)$$

where z is the tip−surface gap width, z_0 is assigned a value of $[\ln(10)]^{-1}$ Å assuming a 10-fold change in tunneling current per angstrom change in tip−surface separation, and I_0 is assigned a value of 5 × 10^9 nA given a set-point current of 0.5 nA and assuming a 10 Å tip−surface gap at that set point. Further, as a reasonable starting point[19,21] we assume that the tip length changes in proportion to the intensity of the incident laser light (i.e., the system can be described by a temperature-independent absorption coefficient, heat capacity, and constant coefficient of thermal expansion). The calculated response of the tunneling current is shown in Figure 2b, where we have adjusted the constant of proportionality to approximate the observed response. This model predicts that the observed effect is consistent with a ±~0.75-Å maximum modulation of the tip height, shown in Figure 2c.

This simple model reproduces the salient features of the experimental result, supporting the conclusion that the modulation of the current is due to photoinduced thermal modulation of the length of the STM tip. First, it is significant that the current excursions above the baseline are significantly larger than those below the baseline. This strong asymmetry of the current modulation with respect to the set point is what is expected for thermal expansion of the tip (Figure 1b), given the exponential dependence of the current on the width of the tip−surface gap (eq 2). In addition, the positions of the sharp spikes in the experimental data are in excellent agreement with those expected for the undersampled interferogram. Deviations of the data from the expected intensity pattern within the envelope of the interferogram are attributed to errors in the optical delay corresponding to submicrometer movements of components in the optical delay lines and to fluctuations in laser power due to motion of the microscope relative to the laser beam.

Several schemes may be considered to minimize or eliminate the current modulation that results from the interferometric laser intensity modulation. For example, one may consider altering the polarization alignment of the beams or decreasing the laser power. Regarding the polarization alignment, we emphasize that the results shown in Figure 2a were obtained with the polarizations of the two interfering beams fixed perpendicular to each other. For parallel-polarized beams the modulation amplitude was so large that it became difficult to prevent the STM tip from crashing into the surface. Rotating the polarization angles from ±45° with respect to the STM tip axis (as was the case for Figure 2a) such that one is polarized parallel and the other perpendicular to the tip axis did not attenuate the modulation any further. This observation is consistent with the facts that (i) the beam polarizations are not 100% pure and (ii) the tip

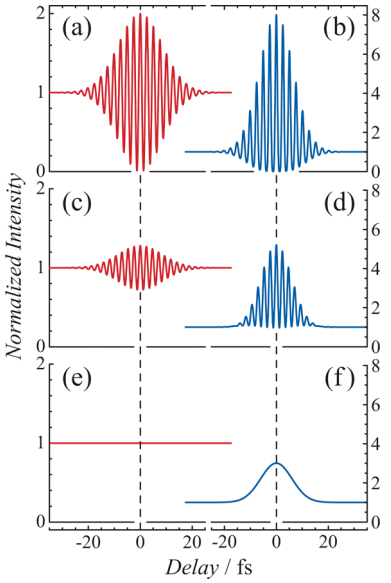

Figure 3. Comparison of the wavelength dependence of the first- and second-order responses of a slow detector to excitation by two FTL pulses with wavelengths λ_1 and λ_2 at variable time delay. Traces (a), (c), and (e) [(b), (d), and (f)] are the first- (second-)order responses (see eq 3). In all cases λ_1 remains fixed at 760 nm; in (a) and (b) λ_2 = 760 nm; in (c) and (d) λ_2 = 660 nm; in (e) and (f) λ_2 = 380 nm. The calculations were performed with two 10-fs fwhm pulses to permit clear display of the fringes.

causes partial depolarization of the light.[33] An alternative approach to minimizing the modulation would be to decrease the laser-pulse fluence. However, decreasing the laser fluence also decreases the peak electronic temperature achieved at the junction, thereby decreasing exponentially the possibility of detecting photoexcited subvacuum hot-electron tunneling. Because the magnitude of the current modulation due to the thermal effect is ~3 orders of magnitude (or more) greater than that expected for photoemission (see results of two-color experiments below), and is similarly greater than what may be anticipated for photoexcited tunneling, decreasing the pulse fluence does not appear to be a viable approach to observing hot-electron dynamics in the junction via these mechanisms.

Related, careful measurements made by Gerstner et al., under similar conditions, have been used to measure the tip expansion.[25] Our results agree with their conclusion that strong thermal effects in the junction make observation of other effects, in particular hot-carrier relaxation dynamics, extremely difficult if not impossible, particularly at time scales of the order of the laser pulse temporal width.[25] We are also convinced that modulation of the delay line, as proposed by Shigekawa and co-workers, does not eliminate these thermal effects. Because the magnitude of the thermal response of the tip decreases with frequency,[20] it has been proposed that thermal effects may be effectively reduced by employing high-frequency and large-amplitude modulation.[12] However, even at large amplitudes (~0.5 ps), modulation in the readily accessible range (10−200 Hz) corresponds to intensity modulations that are quite slow (<200 kHz), compared to the >1 MHz roll-off of the tip response.[20] In addition, dynamics on time scales of the order of the modulation amplitude will be strongly distorted.[14] Consequently, large-amplitude high-frequency modulation is not a solution for measuring dynamics in the sub-~1 ps regime with laser-assisted STM.

B. Two-Color Photoexcited STM. The basis for our solution to the issue of thermal expansion in the STM tunneling gap is the elimination of the interference by employing pump and probe pulses with different wavelengths. The illustrative calculations in Figure 3 show that the interference between the pulses is attenuated if the wavelength of the first pulse, λ_1, differs from that of the second pulse, λ_2. Significantly, for the case where λ_2 = 0.5 λ_1, the interference fringes are completely eliminated. This is readily evident in the interferograms in Figure 3. These show the calculated first- and second-order responses of a slow detector to optical excitation by two Fourier-transform-limited (FTL) Gaussian pulses from a modified Mach−Zehnder interferometer (as in Figure 1) as a function of the delay between the pulses. In the calculation the detector's response time is taken to be much longer than the temporal width of the laser pulse, an assumption that is certainly valid for the detection of laser-induced transients in the STM,[20,21] such that the measured response is proportional to the time-integrated incident intensity. Figure 3 shows the first- and second-order responses, respectively, for three cases: $\lambda_2 = \lambda_1$ in (a) and (b); $\lambda_2 = \lambda_1 - 100$ nm in (c) and (d); and λ_2 = 0.5 λ_1 in (e) and (f). The delay-dependent intensity response is

$$I_n(t_d) = N^{-1} \int_{-\infty}^{\infty} dt \, |\{E_1(t) + E_2(t + t_d)\}^n|^2 \qquad (3)$$

where t_d is the delay time, n = 1 (2) for the first (second) order response, and N is a normalization constant equal to the integral portion of eq 3 for $t_d \rightarrow \infty$ (i.e., $t_d \gg$ the pulse duration). Here, the "order" describes the nonlinearity of the response of system polarization to the electric field amplitude; n = 1 describes a linear (one-photon) process, whereas n = 2 describes a quadratic (two-photon) one. The time-dependent electric field amplitude for pulse m is

$$E_m(t) = \exp(-t^2/2\sigma_E^2) \cos(2\pi c t/\lambda_m) \qquad (4)$$

where m = 1 (2) for the first (second) pulse, c is the speed of light, and σ_E = fwhm/[2(ln 2)$^{1/2}$], where fwhm is the full width at half-maximum of the Gaussian temporal envelope of the electric field intensity of the pulse. The fwhm for each pulse is taken to be equal to 10 fs for ease of viewing the interference fringes in Figure 3.

The heat load on the tip is proportional to the time-integrated field intensity of the incident pulse pair (right-hand side of eq 3 with n = 1). Thus, the attenuation of the interference fringes in the first-order response with increasing difference in wavelength corresponds to a marked decrease in the delay-dependent variation of the thermal load on the junction. Most importantly, the complete elimination of fringes in the first-order response when λ_2 = 0.5 λ_1 indicates that by employing the second harmonic of the Ti:sapphire laser as a probe pulse it is possible to keep the thermal load constant, i.e., independent of pump−probe delay. Thus the thermally induced modulation of the width of the tip−surface gap is eliminated, even within the envelope of the cross-correlation of the pulses. No less significant is the fact that a second-order response remains (Figure 3f), preserving the ability to observe two-color phenomena such as those due to the mixing of one NIR photon and one UVA photon.

To test the viability of the application of a two-color approach to SPPX-STM, we have measured photoemission from a clean and well-characterized Ag(111) surface excited by 760-nm (~100-fs, fwhm) pump and 380-nm (~200-fs) probe pulses, using the STM tip as a proximate anode to collect photoemitted

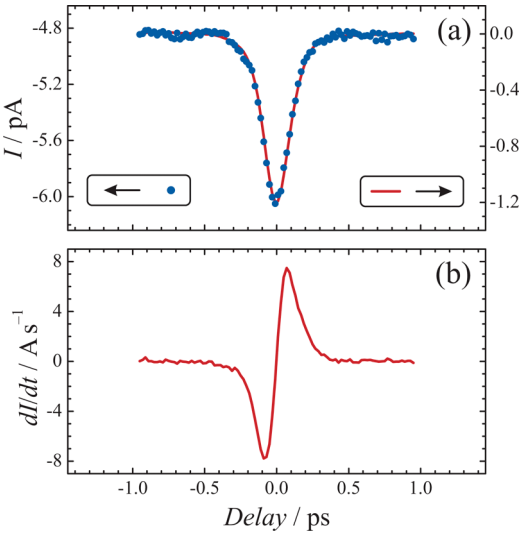

Figure 4. Two-color photoemission from Ag(111) detected with a tungsten STM tip retracted >10 nm from the surface. The filled circles in (a) show the signal recorded directly after current-to-voltage conversion in the STM preamplifier; the trace in (b) is the signal recorded with the lock-in amplifier as explained under Experimental Methods. The solid line in (a) is the integral of the SPPX measurement in (b). The 760-nm, ~100-fs fwhm pulses were cross-correlated with 380-nm, ~200-fs fwhm pulses; the per-pulse fluence was ~16 μJ cm^{-2} NIR + ~28 μJ cm^{-2} UVA. The pump−probe delay was dithered at a frequency ($=\omega_d/2\pi$) of 187 Hz and a peak-to-peak delay amplitude of ~37 fs. The sample bias was −1.0 V, and the base temperature was ~80 K.

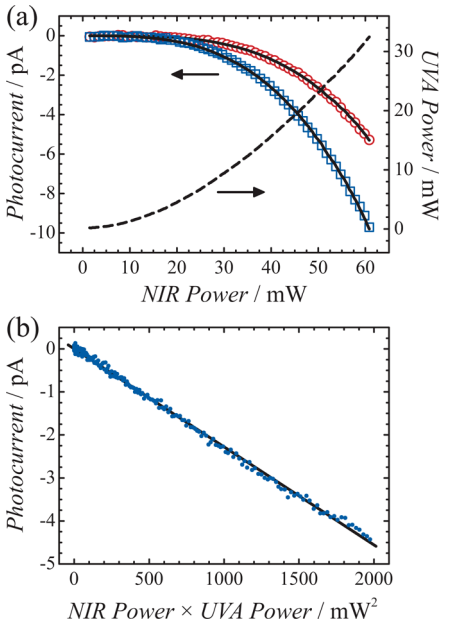

Figure 5. Power dependence of the photoemission yield from Ag(111) detected with a tungsten STM tip retracted >10 nm from the surface. In panel a the abscissa is the NIR power measured at the exit of the interferometer, the dashed line is the corresponding UVA power, and the circles (squares) are the photocurrent signal detected at a pump−probe delay of −1 ps (0 ps). The solid lines are fits of eqs 6 and 7 to the −1- and 0-ps data, respectively. Panel b shows a linear fit (solid line) to the difference between the 0- and −1-ps photocurrent measurements plotted as a function of the product of the NIR and UVA power (see eq 8).

electrons. Figures 4 and 5 show results obtained with the tip retracted a distance of >10 nm from the surface and, therefore, out of tunneling range. The data in Figure 4a confirm that the interference fringes are indeed absent. The current of photoemitted electrons detected by the tip is a smooth Gaussian line shape, similar to the calculated second-order response shown in Figure 3f, with, as expected, no indication of any optical interference.

Figure 4 also shows that dithering the delay is an effective and accurate means of extracting the two-color photoemission from the relatively large one-color background. Our measurements exhibit a delay-independent background signal dominated by photoemission due to the absorption of two UVA photons (see below); specifically, in Figure 4a, the ~ −1.2-pA signal due to two-color photoemission is found to be riding atop an ~ −4.8-pA delay-independent background. Figure 4b shows that the SPPX signal is detected with zero background through the lock-in amplifier, demonstrating the effective elimination of the one-color two-photon photoemission. Furthermore, recovery of the directly detected photoemission current, sans background, by integration of the SPPX signal is shown in Figure 4a, demonstrating the accurate recovery of the delay dependence of the two-color photoemission signal. In order to present the data in units that consistently represent the relationship between the differential (Figure 4b) and integral (Figure 4a, solid line) signals, the data plotted in Figure 4b have been scaled according to

$$\frac{dI_{STM}}{dt_d} = \frac{A_{meas}}{g_{PreAmp}g_{LiA}}\frac{\sqrt{2}}{\Delta t_d} \quad (5)$$

where I_{STM} is the STM current, A_{meas} is the amplitude of the signal recorded by the lock-in amplifier, g_{PreAmp} is the gain of the STM current-to-voltage preamplifier, and g_{LiA} is the lock-in amplifier's amplification factor.

The results of power dependence measurements shown in Figure 5 demonstrate that the observed signal (Figure 4) can be unambiguously assigned to two-color two-photon photoemission and that the background is dominated by photoemission due to the absorption of two UVA photons. These measurements were made by varying the NIR power before sending the beam into the beam sampler (Figure 1), such that a linear increase in the NIR power is accompanied by an approximately quadratic increase in the UVA power (Figure 5a) incident on the surface. The NIR power and UVA power were measured at the exit of the interferometer after being recombined on the dichroic filter but before coupling into the STM. Two distinct photoemission current measurements were made: (i) with the delay between the pulses fixed at −1 ps (the NIR pulse preceding the UVA, Figure 5a, circles) and (ii) with the pulses arriving simultaneously at the surface (Figure 5a, squares). Given the ~4.5 eV work function of Ag(111),[31,32] one-photon photoemission is not possible with λ_1 = 760 nm (1.63 eV) or λ_2 = 380 nm (3.26 eV). The lowest-order energetically allowed processes are (i) 1 UVA photon + 1 NIR photon, (ii) 2 UVA, (iii) 3 NIR, (iv) 2 NIR + 1 UVA, (v) 2 UVA + 1 NIR, and (vi) 3 UVA photoemission. At a pump−probe delay of −1 ps, only processes (ii), (iii), and (vi) are possible. The −1-ps data in Figure 5a (circles) are well fit (solid line through circles) under the assumption that the photoelectron yield depends quadratically on only the incident UVA power; the fit does not require any contribution from a cubic dependence on the NIR or UVA power

and a cubic dependence on either the NIR or UVA power alone does not fit the data. Thus we identify two-UVA-photon photoemission as the predominant process when the pump and probe pulses are not overlapped in time. Figure 5a shows a strong increase in the photoemission yield when the pump and probe pulses are overlapped in time, conceivably due to contributions from processes (i), (iv), and (v). We find that the power dependence of this process is well-fit by addition of a single contribution that is proportional to the product of the UVA and NIR powers (Figure 5a, solid line through squares, and Figure 5b), indicating that only process (i), two-color two-photon photoemission, contributes significantly to the photoemission yield. In summary, the photoemission yields are well-described by

$$Y_{-1\,\mathrm{ps}} = \kappa_1 {P_{\mathrm{UVA}}}^2 \quad (6)$$

and

$$Y_{0\,\mathrm{ps}} = \kappa_1 {P_{\mathrm{UVA}}}^2 + \kappa_2 P_{\mathrm{UVA}} P_{\mathrm{NIR}} \quad (7)$$

where Y_t is the yield at pump−probe delay t, κ_i are proportionality constants, and P_{UVA} and P_{NIR} are the incident UVA and NIR powers. Figure 5b shows that the difference between the two yield curves in Figure 5a scales with the product of the UVA and NIR powers

$$Y_{0\,\mathrm{ps}} - Y_{-1\,\mathrm{ps}} = \kappa_2 P_{\mathrm{UVA}} P_{\mathrm{NIR}} \quad (8)$$

as expected for a two-photon, two-color process. This conclusion is consistent with separate sample-bias dependence measurements (not shown).

Finally, we report the detection of photoexcited electrons with the tip in tunneling range (i.e., within ∼1 nm) of the Ag(111) surface. When two different colors are used as pump and probe (Figure 6a), there is no evidence of the large current oscillations observed in one-color measurements such as those reported here (Figure 2a) and in the work of Gerstner et al.[25] Here, the STM feedback holds the current constant at ∼ −460 pA (Figure 6a). The response time of the z servo loop is ∼2 s, and each data point in each delay scan is averaged for ∼1 s. Under these conditions, strong (∼1 nA) current oscillations such as those in Figure 2a would have resulted in signals readily detectable above the ∼4 pA noise level. The absence of such current oscillations within the cross-correlation envelope of the pulses in the two-color results shown in Figure 6 demonstrates that the thermal modulation of the width of the tip−surface gap has been eliminated. This result represents an important step toward the ultimate goal of simultaneous subnanometer measurements of surface electron dynamics on time scales of the order of the temporal width of the laser pulses, because it shows that the tip can be maintained at a fixed height above the surface throughout the delay sweep and, particularly, in the critical region within ∼±100 fs of zero delay—time scales on which electron−electron, electron−phonon scattering and interfacial electron transfer occur.[34]

Figure 6b shows that a clear two-color response is observed with the tip in tunneling range (top trace). Application of the SPPX approach enables the effective isolation of the ∼3-pA pump−probe cross-correlation signal from the large ∼500-pA background. In what follows, we consider, in turn, three salient features of these data: (i) the relatively large magnitude of the two-color response with the tip in tunneling range compared to out of tunneling range, (ii) the short time scale of the delay-dependent response, and (iii) the marked offset of the baseline.

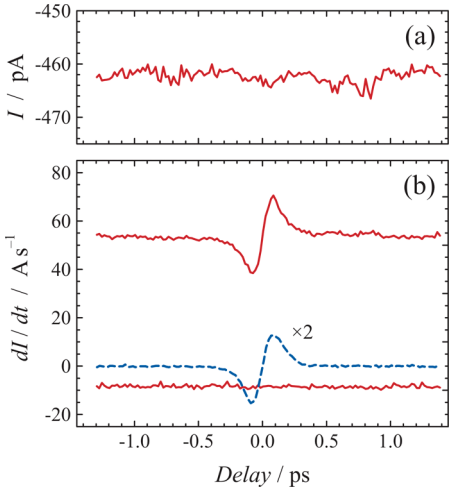

Figure 6. SPPX-STM measurements made with the tip in tunneling range of a Ag(111) surface (solid lines) compared to those made with the tip retracted out of tunneling range (dashed line). Panel a shows the signal recorded directly after current-to-voltage conversion in the STM preamplifier. In (b) SPPX measurements recorded with the lock-in amplifier are shown both with the tip retracted from tunneling range (dashed line) and during tunneling (solid lines). The data during tunneling were collected simultaneously at phase shifts of 0 (top) and $\pi/2$ rad (bottom) with respect to the phase of the tip-retracted case. (Tunneling current set point = 0.5 nA, sample bias = −0.5 V, STM feedback constant = 0.5 Hz, per-pulse fluence ∼23 μJ cm^{-2}, surface temperature = 20 K; the data were recorded over a period of 6 h and are the average of 46 delay scans.)

First, we note that in the particular data set shown in Figure 6b the peak-to-peak amplitude of the response detected in tunneling range (solid line) is about twice that of the response with the tip retracted >10 nm from the surface (dashed line), with all other experimental conditions held constant. We tentatively assign this increase to the enhancement of the optical fields at the surface which is known to increase with decreasing tip−surface gap.[35] In addition, we find that the magnitude of the signal enhancement depends upon the quality and history of the STM tip, presumably due to the transfer of a variable quantity of silver atoms between the Ag(111) surface and the tip apex. Significantly, the presence of field enhancements at the tip apex in combination with the nonlinearity of two-photon photoemission suggests a possible route to spatially resolved two-photon (or higher order) photoemission at the nanoscale. We are currently working to characterize and control the field enhancement.

Second, regarding the time scale of the two-color response, we find a nearly identical temporal width for the two-color response with the tip in tunneling range as that observed with the tip retracted. The similarity of the two results is illustrated in Figure 7, where we have overlaid the same function, the first derivative of a Gaussian with a fwhm of 220 fs, on both data plots. Nonlinear-least-squares fitting gives the fwhm's for the responses observed with the tip retracted from (Figure 7a) and engaged in (Figure 7b) tunneling to be 218 ± 2 fs and 212 ± 4 fs, respectively. Thus the time scales of both measurements are consistent with normal two-photon photoemission from the Ag(111) surface at the photon energies we employ. Specifically, we expect that the emission is dominated by coherent two-photon photoexcitation across the well-known gap in the ΓL-projected density of states (DOS).[36−38] Possible photoemission contributions

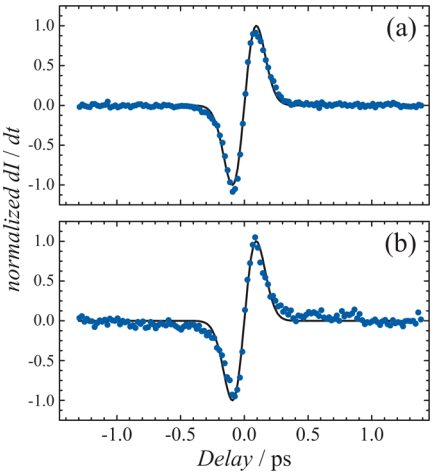

Figure 7. SPPX-STM data from Figure 6 normalized to a peak-to-peak signal amplitude of 2. Panels a and b are measurements made with the tip retracted from and engaged in tunneling, corresponding to the dashed and solid lines in Figure 6, respectively. The derivative of a 220-fs fwhm Gaussian is overlaid on both data sets.

from real intermediate states will involve electrons from ~1.2 eV above the Fermi level or higher, and therefore involve (according to Fermi liquid theory) lifetimes no greater than ~18 fs.[39,40] Thus, given the temporal resolution of our setup (~20 fs), we expect no detectable contribution of any finite lifetime from real intermediate states to the tip-retracted measurement, and the resulting fwhm is equal to the cross-correlation of the two pulses. That the width observed with the tip engaged in tunneling is, within experimental uncertainty, the same as that with the tip retracted, indicates that there is no significant contribution to the photoexcited tunneling signal that could be assigned to a real intermediate state with a lifetime of >~20 fs. Thus we conclude that we do not observe finite lifetimes associated with secondary electrons that have relaxed to intermediate states close to the Fermi level. Such electrons can comprise a significant component of photoemitted electrons in energy-resolved two-photon photoemission measurements at higher photon energies than employed here.[39−42] At the photon energies used here an analogous contribution from photoassisted tunneling of subvacuum electrons from states with lifetimes in the ~20-fs range is energetically allowed; however, these are not distinguished from photoemitted electrons because of our limited temporal resolution. Furthermore, the ΓL gap limits these to a narrow energy range, thereby limiting the magnitude of their contribution.[40] We are designing experiments that enhance the relative contribution of electrons from intermediate states close to the Fermi level where the electron lifetimes are significantly longer. The possibility of detecting these electrons *only* when the tip is in tunneling range would, if realized, represent another significant step toward the goal of measuring surface electron dynamics with simultaneous subnanometer and subpicosecond resolution.

Finally, Figure 6b shows a marked offset of the baseline of the signal detected in tunneling range. This offset consists of two components: a large ~54 A s^{-1} offset phase shifted by π with respect to the subpicosecond transient (evidenced in the large positive offset of the top trace in Figure 6b), and a smaller ~8.5 A s^{-1} offset phase shifted by $\pi/2$ (i.e., detected in the "quadrature" channel, bottommost trace in Figure 6b). These offsets are consistent with a sinusoidal modulation of the tunneling current whose amplitude is independent of delay and whose phase is fixed with respect to that of the dither. This conclusion is reached by considering the two conceivable causes of a constant offset: (i) a baseline that increases linearly (i.e., has a constant slope) with delay or (ii) a sinusoidal current oscillation driven by the UVA retroreflector modulation. We rule out possibility (i) on the basis of two considerations: first, in tip-retracted measurements where the delay is not modulated we see no evidence of the very large (~50 pA ps^{-1}) slope that would be required to explain the observed offset; second, a linearly increasing baseline would require a seemingly unphysical response—in particular, the observed lack of antisymmetry of the sign of the offset with respect to zero delay is inconsistent with what we would expect, for example, from a slow (~100 ps) response associated with a delay-dependent thermal expansion.

On the other hand, explanation (ii), a sinusoidal oscillation driven by the modulation, seems quite likely. There are at least two possible sources of such a modulation. First, a small (submicrometer) periodic deviation of the UVA beam position due to changes in alignment accompanying the motion of the dithering retroreflector could result in a modulation of the one-color two-photon background at the frequency of the dither that would add a constant offset. Second, periodic deviation of the UVA beam (or the NIR beam, or both), due to vibrations attendant with the motion of the dithering retroreflector, would also result in a modulation in the thermal load on the tip; the resultant modulation of the STM current would occur at a fixed phase delay resulting in a signal in the quadrature channel. That the phase lag we observe is consistent (modulo π) with that observed by Grafström et al.[20] may suggest that the thermal effect is dominant. If so, the additional π shift we observe would indicate that the beam deviation responsible for the thermal load modulation is π out of phase with the delay dither. While further work is required to specify the source of the observed offsets, the data are readily explained by photoinduced thermal expansion and contraction of the tip resulting from small variations in alignment and laser spot size accompanying the modulation of the path length. We expect that these variations will be difficult to completely eliminate. Finally, we note that the data in Figure 6 were processed directly according to eq 5 for the purpose of comparison to the data recorded with the tip retracted. However, having identified the offset as due to a constant modulation and not to a delay-dependent response, it is not correct to interpret the offset as a slope; instead, subtraction of the offset from the data prior to conversion to amperes per second would be justified.

C. Comparison with Other Recent Advances. The advantage of the two-color approach that we are introducing here can be appreciated more fully by direct comparison with two other recent advances in ultrafast time-resolved STM. First, we consider in fuller detail the work of Shigekawa and co-workers mentioned above. In early work, this group implemented a one-color 2PC approach in an attempt to observe subpicosecond surface electron dynamics in nitrogen-doped GaAs. They reported time constants derived from laser-assisted SPPX-STM of 1,[12] 50,[12] 118,[16] 550,[16] and 440 ps[30] for the same material. Only the latter two agree, within experimental uncertainty, with the 410-ps lifetime derived from transient reflectivity measurements described in the most recent reports.[16,30] Based on our one-color results, as well as those of Gerstner et al.,[25] and the analysis presented by Takeuchi et al.,[14] we believe that the shortest relaxation time derived from the early SPPX measurement does not represent transient electron dynamics but, rather, the result

of thermal effects due to optical interference. Despite the efforts made to minimize the optical interference by modulating the delay, these effects appear to be difficult, if not impossible, to eliminate while preserving the desired signal in the subpicosecond range.

Within the context of a one-color SPPX measurement, possible approaches to minimizing the impact of optical interference involve the following: (i) decreasing the laser power, (ii) increasing the amplitude of the dither, (iii) increasing the frequency of the delay dither, and (iv) decreasing the laser pulse width. At this stage it is difficult to make conclusive quantitative statements regarding the viability of these approaches, but some qualitative generalizations can be made.

First, decreasing the laser power is undesirable because it will result in a decrease in the signal-to-noise ratio in these already challenging measurements. Second, increasing the amplitude of the delay modulation, though it effectively increases the frequency of the interferometric intensity modulation (thereby potentially decreasing the response of the tip[20]), is also undesirable because it decreases the temporal resolution—the larger the delay modulation amplitude, the larger the range of delay times over which the pulses overlap during the dither and, consequently, the larger the delay range over which the interferometric intensity modulation is of concern, increasing the temporal "blind spot" that is of the order of the delay dither amplitude. This consideration may explain why the shortest time constant (1 ps) observed in the earliest experiments[12] was of the time scale of the dither amplitude (0.7−0.5 ps[12,14]), as well as why this fast decay was not detected in later experiments on the same material where the delay modulation amplitude was increased to 6 ps.[16] Calculations by Takeuchi et al.[14] suggest that, even with a pulse width of 25 fs, dithering the pulses creates the potential for thermal effects in the range of delay times $-\Delta t_d < t_d < +\Delta t_d$. Because the thermal effects result in signals orders of magnitude larger than those desired, it seems unlikely that they can be eliminated from making significant, if not dominant, contributions within this delay range.

Third, increasing the frequency of the delay dither seems attractive until one realizes that the intensity modulation frequency approaches zero near the turning points of the delay dither by virtue of the fact that the dither is sinusoidal. Thus, there will always be a range of delays over which there is a very slow modulation of the laser intensity to which the tip will be highly sensitive. Finally, narrowing the pulse width beyond 25 fs is feasible; however, the temporal resolution will remain limited by the dither amplitude. Optimizing the temporal resolution thus would involve decreasing the dither amplitude which would decrease the signal-to-noise ratio, increase data acquisition times, and, again, make these already challenging measurements all the more difficult.

Indeed, after nearly a decade of effort, Shigekawa and coworkers seem to have concluded that sinusoidal dithering is not the optimal means to eliminate thermal effects in laser-assisted STM. Very recently they reported implementation of an exciting new approach that involves pulse picking to generate a clean square-wave delay modulation, effectively chopping the delay in a "binary" mode between a fixed long delay (approximating an infinite delay) and a variable finite delay which is scanned to measure carrier relaxation dynamics.[30] The advantages of this approach are (i) the delay can be chopped at a higher frequency than accessible to mechanical dithering, moving the experiment into a quieter region of the noise spectrum; (ii) the detected signal is equal to the total magnitude of the effect above the background tunneling current (and no longer limited by the amplitude of the dither), resulting in an order of magnitude increase in signal levels; and (iii) the delay range can be extended from a few picoseconds to the microsecond range; thus a wide range of lifetimes of electronic excitations can be probed with subnanometer spatial resolution. The disadvantage is that, as implemented, the temporal resolution is limited by the 600-fs timing jitter in the scanning of the delay which is achieved electronically through synchronization of the pulse trains of two Ti:sapphire lasers. In principle, a modified, all-optical-delay version of this approach may enable access to shorter time scales, but the fastest dynamics reported in the most recent work are in the few picoseconds range.[30] Furthermore, we believe that optical interference in a one-color setup will continue to create a "blind spot" over the range of delay times falling within the autocorrelation temporal envelope; thus, an ideal next step would combine our two-color approach with this "binary" delay chopping technique, permitting unfettered access to subpicosecond dynamics on the nanoscale.

In another very recent and related effort, Wu and Ho have reported measurements of the photoinduced transfer of an electron from an STM tip to a single porphine molecule adsorbed on a thin insulating film on a metal surface.[28] In this work two-photon absorption in a tip irradiated with ∼70 fs pulses at ∼800 nm promotes electrons to energies up to ∼3.1 eV above the Fermi level of the tip. This lowers the effective barrier to tunneling; thus photoexcited electrons can tunnel to high-lying unoccupied molecular orbitals of the porphine—e.g., the LUMO (lowest unoccupied molecular orbital) + 1—at biases where nonphotoexcited tunneling electrons cannot. In a first attempt to explore the possibility of using this unique setup to time resolve the dynamics of charge transfer from an STM tip to a surface, Wu and Ho conducted 2PC measurements. To avoid thermal effects due to optical interference of the pulses, the delay was sinusoidally dithered (by a method similar to that used in our experiments) with a peak-to-peak amplitude equal to one optical cycle. Nevertheless, because the frequency of the dither was limited to ∼100 Hz, the measurements were constrained to be performed at very low laser power (<0.2 mW) in order to minimize current oscillations due to the modulation of the thermal load on the junction that was induced by optical interference.

The results of Wu and Ho illustrate that it may be possible to time resolve phenomena in the junction on time scales of the order of laser pulse. It is important to note that their approach is thus far only seen as possibly appropriate to probing electron dynamics *in the STM tip* and in essence uses a carefully designed electronically isolated (and, therefore, very long-lived) single molecule system as an electron detector.[43] It does not yet appear to be appropriate to the generalized probing of spatially resolved dynamics of electrons in surfaces. In addition, the authors are appropriately tentative in their interpretations of their time-resolved data[28] for at least two reasons: (i) it remains to be determined what contribution the thermal oscillations of the tip make to the observed signals and (ii) the signal-to-noise levels in these challenging experiments are quite low. By incorporating a method similar to our two-color approach, these single molecule charging experiments could be performed under conditions where the thermal load is held constant by natural averaging over the optical cycle (as illustrated in Figure 3e); thus no dither would be required and the experiments could be performed at higher laser power without introducing tip-length oscillations. We

expect that this would dramatically improve the signal-to-noise ratio in these experiments and greatly facilitate their time-resolving capability as well as their interpretation.

4. CONCLUSION

We report progress in our work aimed at developing an ultrafast (subpicosecond) time-resolved local probe of electron dynamics using the STM tip as a proximate anode. We discuss results obtained using two distinct methods: (i) a one-color two-pulse correlation approach and (ii) a new two-color pump−probe approach. We show that the two-color approach holds promise for application to fast subpicosecond dynamics, on time scales of the order of the laser pulse width, where the one-color approach is unsuitable.

Specifically, we find that signals in attempted one-color measurements are dominated by temporal-interference-induced angstrom-level thermal modulations of the width of the tip−surface gap. Our experiments suggest that the original one-color implementation of the SPPX method[11,12] does not circumvent the thermal modulation problems, confirming the results of Gerstner et al.[25] and calling into question the claim that subpicosecond electron dynamics measurements—on time scales of the order of the sum of the width of the laser pulses and the amplitude of the delay dither—have been achieved by Takeuchi et al.[12]

We have made a significant step toward the goal of probing nanoscale surface electron dynamics by implementing our new approach: two-color laser-assisted STM. The two-color approach completely avoids temporal interference and opens the possibility of detecting transient electronic excitations on time scales comparable to the pump−probe cross-correlation envelope. Application of the SPPX method,[11,12] involving dithering the pump−probe delay, is demonstrated to be an effective and accurate means of extracting the two-color photoemission from the relatively large one-color two-photon background. The transient photoemission signal detected with the tip retracted ∼10 nm from the surface is solidly assigned to two-color two-photon photoemission based on the power dependence of the photoemission intensity.

Finally, we report the detection of photoexcited electrons with the tip in tunneling range of the surface. The SPPX method is found to effectively isolate the relatively small photoexcited current from the much larger conventional tunneling current. The measurements are accomplished without any indication of pump−probe-delay-dependent thermal modulations. The results indicate that our approach is capable, in principle, of simultaneous temporal and spatial resolution of surface electron dynamics. Further investigations aimed at exclusively measuring photoexcited tunneling and utilizing field enhancements at the STM probe tip to achieve nanometer-scale spatially resolved photoemission are underway.

AUTHOR INFORMATION

Corresponding Author

*E-mail: nicholas@bnl.gov.

Present Addresses

[§]Center for Nano & Molecular Science, The University of Texas at Austin, Austin, TX 78712, United States.

[∥]Fundamental and Computational Sciences Directorate, Institute for Interfacial Catalysis, Pacific Northwest National Laboratory, Richland, WA 99352, United States.

ACKNOWLEDGMENT

We gratefully acknowledge M. G. White and J. Zhou for their help with frequency doubling. We also thank G. Hall and A. Harris for helpful discussions. The experiments were carried out at the Center for Functional Nanomaterials, a Nanoscale Science Research Center supported by the Office of Basic Energy Sciences, U.S. Department of Energy. The research was supported by the U.S. Department of Energy, Office of Basic Energy Sciences, Division of Chemical Sciences, under Contract No. DE-AC02-98CH10886 as part of a Chemical Imaging initiative within the Catalysis Science Program.

REFERENCES

(1) *Laser Spectroscopy and Photochemistry on Metal Surfaces, Part II*; Dai, H.-L., Ho, W., Eds.; World Scientific: Singapore, 1995.
(2) Nienhaus, H. *Surf. Sci. Rep.* **2002**, *45*, 1.
(3) Maximoff, S. N.; Head-Gordon, M. P. *Proc. Natl. Acad. Sci. U.S.A.* **2009**, *106*, 11460.
(4) Park, J. Y.; Lee, H.; Renzas, J. R.; Zhang, Y.; Somorjai, G. A. *Nano Lett.* **2008**, *8*, 2388.
(5) Binning, G.; Rohrer, H.; Gerber, Ch.; Weibel, E. *Phys. Rev. Lett.* **1982**, *49*, 57.
(6) Grafström, S. *J. Appl. Phys.* **2002**, *91*, 1717.
(7) Hamers, R. J.; Cahill, D. G. *Appl. Phys. Lett.* **1990**, *57*, 2031.
(8) Feldstein, M. J.; Vöhringer, P.; Wang, W.; Scherer, N. F. *J. Phys. Chem.* **1996**, *100*, 4739.
(9) Pfeiffer, W.; Sattler, F.; Vogler, S.; Gerber, G.; Grand, J.-Y.; Möller, R. *Appl. Phys. B: Laser Opt.* **1997**, *64*, 265.
(10) Merschdorf, M.; Pfeiffer, W.; Thon, A.; Gerber, G. *Appl. Phys. Lett.* **2002**, *81*, 286.
(11) Takeuchi, O.; Morita, R.; Yamashita, M.; Shigekawa, H. *Jpn. J. Appl. Phys.* **2002**, *41*, 4994.
(12) Takeuchi, O.; Aoyama, M.; Oshima, R.; Okada, Y.; Oigawa, H.; Sano, N.; Shigekawa, H.; Morita, R.; Yamashita, M. *Appl. Phys. Lett.* **2004**, *85*, 3268.
(13) Shigekawa, H.; Takeuchi, O.; Aoyama, M. *Sci. Technol. Adv. Mater.* **2005**, *6*, 582.
(14) Takeuchi, O.; Aoyama, M.; Shigekawa, H. *Jpn. J. Appl. Phys.* **2005**, *44*, 5354.
(15) Takeuchi, O.; Aoyama, M.; Kondo, H.; Taninaka, A.; Terada, Y.; Shigekawa, H. *Jpn. J. Appl. Phys.* **2006**, *45*, 1926.
(16) Terada, Y.; Aoyama, M.; Kondo, H.; Taninaka, A.; Takeuchi, O.; Shigekawa, H. *Nanotechnology* **2007**, *18*, 044028.
(17) Shigekawa, H.; Yoshida, S.; Takeuchi, O.; Aoyama, M.; Terada, Y.; Kondo, H.; Oigawa, H. *Thin Solid Films* **2008**, *516*, 2348.
(18) Groeneveld, R. H. M.; van Kempen, H. *Appl. Phys. Lett.* **1996**, *69*, 2294.
(19) Grafström, S.; Kowalski, J.; Neumann, R.; Probst, O.; Wörtge, M. *J. Vac. Sci. Technol., B* **1991**, *9*, 568.
(20) Grafström, S.; Schuller, P.; Kowalski, J.; Neumann, R. *J. Appl. Phys.* **1998**, *83*, 3453.
(21) Gerstner, V.; Thon, A.; Pfeiffer, W. *J. Appl. Phys.* **2000**, *87*, 2574.
(22) Ukraintsev, V. A.; Yates, J. T., Jr. *J. Appl. Phys.* **1996**, *80*, 2561.
(23) Lyubinetsky, I.; Dohnálek, Z.; Ukraintsev, V. A.; Yates, J. T., Jr. *J. Appl. Phys.* **1997**, *82*, 4115.
(24) Geshev, P. I.; Klein, S.; Dickmann, K. *Appl. Phys. B: Laser Opt.* **2003**, *76*, 313.
(25) Gerstner, V.; Knoll, A.; Pfeiffer, W.; Thon, A.; Gerber, G. *J. Appl. Phys.* **2000**, *88*, 4851.
(26) Budde, F.; Heinz, T. F.; Loy, M. M. T.; Misewich, J. A.; de Rougemont, F.; Zacharias, H. *Phys. Rev. Lett.* **1991**, *66*, 3024.
(27) Anisimov, S. I.; Kapeliovich, B. L.; Perel'man, T. L. *Sov. Phys. JETP* **1974**, *39*, 375.
(28) Wu, S. W.; Ho, W. *Phys. Rev. B* **2010**, *82*, 085444.
(29) Spanakis, E.; Chimmalgi, A.; Stratakis, E.; Grigoropoulos, C. P.; Fotakis, C.; Tzanetakis, P. *Appl. Phys. Lett.* **2006**, *89*, 013110.

(30) Terada, Y.; Yoshida, S.; Takeuchi, O.; Shigekawa, H. *Nat. Photonics* **2010**, *4*, 869.
(31) Chelvayohan, M.; Mee, C. H. B. *J. Phys. C: Solid State Phys.* **1982**, *15*, 2305.
(32) Giesen, K.; Hage, F.; Himpsel, F. J.; Riess, H. J.; Steinmann, W. *Phys. Rev. Lett.* **1985**, *55*, 300.
(33) Gucciardi, P. G.; Lopes, M.; Déturche, R.; Julien, C.; Barchiesi, D.; Lamy de la Chapelle, M. *Nanotechnology* **2008**, *19*, No. 215702.
(34) Petek, H.; Ogawa, S. *Prog. Surf. Sci.* **1997**, *56*, 239.
(35) Behr, N.; Raschke, M. B. *J. Phys. Chem. C* **2008**, *112*, 3766.
(36) Hansson, G. V.; Flodström, S. A. *Phys. Rev. B* **1978**, *17*, 473.
(37) Nelson, J. G.; Kim, S.; Gignac, W. J.; Williams, R. S.; Tobin, J. G.; Robey, S. W.; Shirley, D. A. *Phys. Rev. B* **1985**, *32*, 3465.
(38) Pontius, N.; Sametoglu, V.; Petek, H. *Phys. Rev. B* **2005**, *72*, No. 115105.
(39) Ogawa, S.; Nagano, H.; Petek, H. *Phys. Rev. B* **1997**, *55*, 10869.
(40) Knoesel, E.; Hotzel, A.; Wolf, M. *Phys. Rev. B* **1998**, *57*, 12812.
(41) Ogawa, S.; Petek, H. *Surf. Sci.* **1996**, *357*, 585.
(42) Knoesel, E.; Hotzel, A.; Hertel, T.; Wolf, M.; Ertl, G. *Surf. Sci.* **1996**, *368*, 76.
(43) Wu, S. W.; Ogawa, N.; Ho, W. *Science* **2006**, *312*, 1362.